Express Polymer Letters Vol.17, No.1 (2023) 54–68
Available online at www.expresspolymlett.com
https://doi.org/10.3144/expresspolymlett.2023.5

Research article

Photocuring and digital light processing 3D printing of vitrimer composed of 2-hydroxy-2-phenoxypropyl acrylate and acrylated epoxidized soybean oil

Sigita Grauzeliene[1], *Brigita Kazlauskaite*[1], *Edvinas Skliutas*[2], *Mangirdas Malinauskas*[2], *Jolita Ostrauskaite*[1*]

[1]Department of Polymer Chemistry and Technology, Kaunas University of Technology, Radvilenu Rd. 19, LT-50254 Kaunas, Lithuania
[2]Laser Research Center, Faculty of Physics, Vilnius University, Sauletekio Ave. 10, LT-10223 Vilnius, Lithuania

Received 26 May 2022; accepted in revised form 22 August 2022

Abstract. Vitrimers have gained attention as materials with recyclability, self-healing, and shape memory properties. The use of bio-based monomers for the synthesis of vitrimers is relevant because of the use of an environmentally friendly strategy. In this work, resins based on 2-hydroxy-2-phenoxypropyl acrylate and acrylated epoxidized soybean oil were designed and tested by real-time photorheometry, Fourier transform infrared spectroscopy (FT-IR), and mechanical testing to determine suitability for digital light processing 3D printing. The synthesis of vitrimer that could have good thermal properties and vitrimeric abilities, such as shape memory, self-healing, and recyclability properties, was investigated. Because of this, the vitrimer could repair cracks and defects and could have a complex design of several parts, which also contributes to recyclability and decreases costs. The rigidity and viscosity of the resins were reduced with an increasing amount of 2-hydroxy-2-phenoxypropyl acrylate-based monomer. The resin that has the highest amounts of hydroxyl and ester groups that are beneficial for transesterification reactions was chosen for vitrimer synthesis in order to show vitrimeric abilities such as self-healing, shape memory properties, reprocessability, and recyclability. The synthesized vitrimer was applied to digital light processing 3D printing and showed shape memory with a recovery ratio of 100%, self-healing and reprocessability with an efficiency of 47 and 31% and recyclability properties.

Keywords: *smart polymers, biobased, rheology, vitrimers, glycerol, DLP 3D printing*

1. Introduction

The attention of polymeric materials researchers is turned towards non-recyclable and non-reshapable thermosets such as Bakelite as a challenge to develop cross-linked polymers that have controllable reprocessing due to dynamic covalent bonds that bridge the gap between thermoplastics and thermosets [1]. Dynamic covalent bonds are bonds with advantages over common covalent bonds as they split into reversible groups, which can be sufficiently reconstructed [2]. These dynamic bonds also provide unique features such as self-healing, weldability, malleability, recyclability, and shape memory properties for polymeric materials [3]. The most recently studied vitrimers based on dynamic covalent bonds are epoxy-based, relying on reversible transesterification reactions [4]. A self-healing property allows repair of cracks and defects, as well as due to weldability, polymeric materials can have complex design from several parts, which also contributes to recyclability by promoting sustainable resource management and decreasing costs [5]. Many reversible reactions, such

*Corresponding author, e-mail: jolita.ostrauskaite@ktu.lt

as transamination, boronic esters-based exchanges, urethane reversion, vinylogous urethane exchange, *etc*., have been used to design dynamic covalent bonds [6], but the most widely studied is the thermoactivated transesterification reaction of hydroxyl and ester groups [7]. The first covalently cross-linked networks based on reversible transesterification exchange reactions were introduced by Leibler and coworkers and were termed 'vitrimers' as they behave like vitreous silica and rearranged their topology without depolymerization, as well as being insoluble and reprocessable [8]. Vitrimers demonstrate two glass transition temperatures T_g and T_v [9]. Below T_v (topology freezing temperature), vitrimers behave as permanently cross-linked thermosets, and above T_v, exchange reactions within their network accelerate, making viscoelastic flow possible, following the Arrhenius law [10, 11]. T_g can be controlled by changing the composition of the resin [12], while T_v occurs due to reversible reactions and can be controlled by changing the transesterification catalyst and its concentration [9]. The catalysts most commonly used for vitrimer synthesis are organometallic complexes and organic bases, such as triazabicyclodecene and zinc acetylacetone hydrate ($Zn(acac)_2$) [13, 14]. However, these catalysts have poor solubility, which can be a drawback for the optical 3D printing process. Schlögl and co-workers have introduced organic phosphates and phosphonates as transesterification catalysts that were soluble in acrylate monomers and allowed efficient stress relaxation of the materials at higher temperatures, which is important for the reshaping and repair of 3D printed objects [15–17].

In the last five years, an increase in scientific publications with biobased vitrimers has been observed. Functionalized triglycerides, lignin, vanillin, tannin, polysaccharides, and furan derivatives have already been used as monomers for various vitrimer synthesis reactions [6]. This attracts the attention of the vitrimer researchers to the need to develop new bio-based monomers for the synthesis of high-performance and sustainable materials. Biodiesel production from vegetable oils and animal fats generates approximately 10% (w/w) of glycerol as the main by-product, which has been used as a starting material for the synthesis of various glycerol-based monomers [18]. Glycerol is a low volatile, non-toxic, hygroscopic monomer compatible with a wide range of materials, miscible monomer with plasticizing effect [19] and has even been used to produce biodegradable plastics already [20–22], which is attractive for vitrimer synthesis. Commercially available glycerol-based monomers, such as 2-hydroxy-2-phenoxypropyl acrylate (HPPA), glycerol 1,3-diglycerolate diacrylate, 3-(acryloyloxy)-2-hydroxypropyl methacrylate, have been used for the synthesis of vitrimers by optical 3D printing since they have hydroxyl and ester groups which are essential for transesterification reactions [15–17, 23, 24]. The obtained vitrimers had shape memory and self-healing properties, and were reprocessable. However, these glycerol monomers were cross-linked mainly with petroleum-based monomers. Moreover, the lack of bio-based resins suitable for digital light processing (DLP) 3D printing of vitrimers led to the development of a novel vitrimer based on glycerol and soybean oil for DLP 3D printing. At the same time, the novel plant-based resins offer a high renewable carbon content and can be used for various optical lithography setups enabling 3D printing on multiple scales [25].

Vegetable oils and their derivatives, such as fatty acids, have been used for vitrimer synthesis, because their price is low, they are easily modifiable, and vitrimers can have properties such as flexibility, resistance to chemicals, low toxicity, and biodegradability [26–30]. Most of the time, epoxidized vegetable oils with carboxylic acids were used for vitrimer synthesis, as carboxylic acid groups act as catalysts for transesterification [31–34]. Acrylated epoxidized soybean oil (AESO) was thermally cross-linked with a dithiol with a boronic ester linkage as a dynamic bond [11]. The synthesized vitrimer was prepared by an environmentally friendly strategy and had self-healing and reprocessability properties.

The aim of this work was to develop and investigate new vitrimers based on glycerol and soybean oil suitable for optical 3D printing. Vitrimers were synthesized using an environmentally friendly strategy by mixing the monomers at different ratios with a photoinitiator and transesterification catalyst and applying irradiation under solvent-free conditions. 2-Hydroxy-2-phenoxypropyl acrylate (HPPA) (Figure 1) was chosen as a monomer as has the glycerol fragment in the structure with hydroxyl and ester groups that are essential for the transesterification reaction. Acrylated epoxidized soybean oil (AESO) was chosen as a cross-linker because of the functional groups of hydroxyl and ester and is reported here for the first time in UV-curable resins for the synthesis of vitrimers.

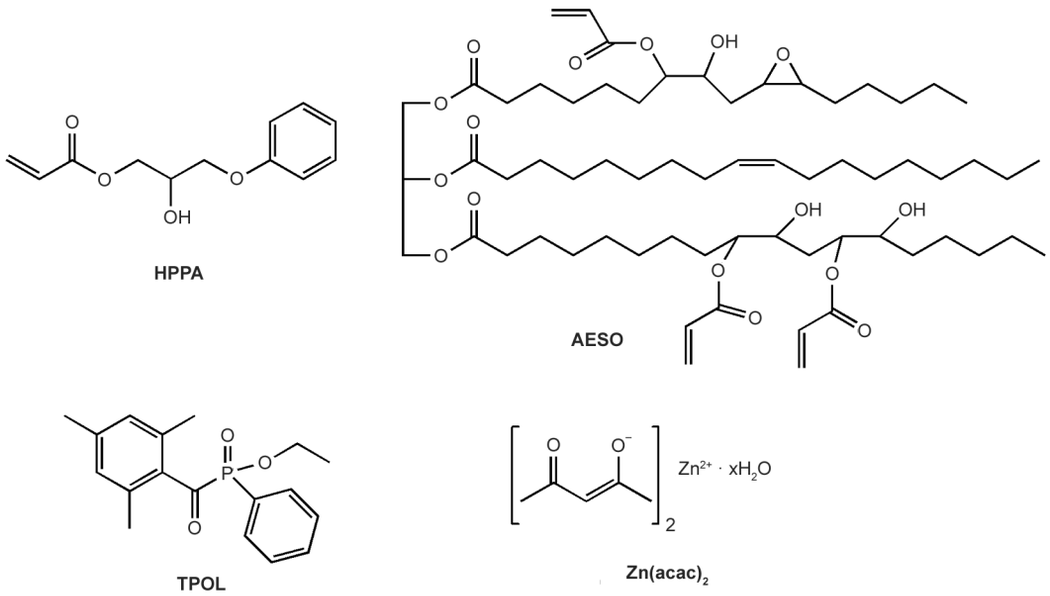

Figure 1. Chemical structures of 2-hydroxy-2-phenoxypropyl acrylate (HPPA), acrylated epoxidized soybean oil (AESO), ethyl(2,4,6-trimethylbenzoyl) phenylphosphinate (TPOL) and zinc acetylacetone hydrate ($Zn(acac)_2$).

Ethyl(2,4,6-trimethylbenzoyl) phenylphosphinate (TPOL) was used as a photoinitiator as allows to get transparent coatings due to the photobleaching effect [35, 36]. Zinc acetylacetone hydrate ($Zn(acac)_2$) was used as a transesterification catalyst, which is one of the most commonly used catalysts and is soluble in the selected acrylate monomers. The rheological properties and photocuring kinetics of the resins based on glycerol and soybean oil were monitored for the first time. The experiments showed the influence of the amount of functionalized glycerol monomer on the viscosity and rheological properties. AESO was found to be a suitable cross-linker in the UV-curing reactions with HPPA because after UV-curing, the dynamic networks were able to rapidly undergo thermoactivated rearrangements of the network topology, as shown by stress relaxation experiments. Incorporation of AESO in the resins with HPPA led to self-healing, shape memory properties, reprocessability, and recyclability. The novel resin based on glycerol and soybean oil was used to form vitrimeric 3D structures by DLP 3D printing.

2. Experimental

2.1. Materials

2-Hydroxy-2-phenoxypropyl acrylate (HPPA, ≥80%), soybean oil, epoxidized acrylate (AESO, ≤100%), and zinc acetylacetone hydrate ($Zn(acac)_2$, ≤100%) were purchased from Merck, Darmstadt, Germany. Ethyl(2,4,6-trimethylbenzoyl) phenylphosphinate (TPOL, >95%) was purchased from Fluorochem, Hadfield, Derbyshire, United Kingdom. All chemicals were used as received.

2.2. Preparation of UV-curable resins

The resins were prepared by dissolving 5 mol% of transesterification catalyst $Zn(acac)_2$ in HPPA at 70 °C. After the resin was cooled down to room temperature, different amounts of AESO and 3 mol% of TPOL were added as the photoinitiator with respect to the total amount of both monomers and stirred at room temperature. The resin codes consist of a number that expresses the amount of HPPA (0–100 wt%) and the abbreviation of 2-hydroxy-2-phenoxypropyl acrylate (HPPA), *e.g.*, 9HPPA is a resin with the weight ratio of 9:1 of monomer HPPA and cross-linker AESO. 9HPPAV is a post-cured vitrimer at 200 °C for 4 h.

The viscosity of the resins based on glycerol and soybean oil was measured with an Anton Paar rheometer MCR302 (Graz, Austria) with a plate/plate accessory (15 mm diameter of the top plate) using a shear rate of 0.001 to 50 s^{-1} at 25 °C.

Resins were cross-linked in a Teflon mold of size of (70×10×1)±0.01 mm under a 500 W Helios Italquartz GR.E UV lamp (Milano, Italy) at a wavelength of 250–450 nm and an intensity of 310 $mW \cdot cm^{-2}$ for 2 min until a solid polymer was obtained.

2.3. Characterization techniques

The photocuring kinetics of the resins was studied using an Anton Paar MCR302 (Graz, Austria)

Table 1. Composition of resins based on glycerol and soybean oil.

Resin	Amount of HPPA [wt%]	Amount of AESO [wt%]	Amount of TPOL [mol%]	Amount of $Zn(acac)_2$ [mol%]	Viscosity [mPa·s]
0HPPA	–	100	3	5	24862±240
1HPPA	10	90			11650±137
2HPPA	20	80			7969±135
3HPPA	30	70			6210±66
4HPPA	40	60			3998±35
5HPPA	50	50			1885±14
6HPPA	60	40			1633±3
7HPPA	70	30			1403±29
8HPPA	80	20			423±11
9HPPA	90	10			332±7
10HPPA	100	–			184±4

rheometer with plate/plate accessory and the Omni-Cure S2000 curing system from Lumen Dynamics Group Inc. (Mississauga, Ontario, Canada). The diameter of the bottom glass plate and the top steel plate was 38 and 15 mm, respectively. The tests were carried out at a temperature of 25 °C and a resin thickness of 0.1 mm. The resins were irradiated with UV/VIS radiation with a wavelength of 250–450 nm and an intensity of 9.3 $W \cdot cm^{-2}$ through a bottom glass plate. A shear test was performed using a frequency of 10 Hz and a strain of 0.5%. The values of the storage modulus G', loss modulus G'', and the complex viscosity η^* of the resins were determined after 120 s of irradiation. The gel point t_{gel} was identified as the crossover point of the G' and G'' modulus curves. The shrinkage was defined as the difference between the gap before and after photocuring.

Fourier transformation infrared (FT-IR) reflection spectra were recorded using a Spectrum BX II FT-IR spectrometer (Perkin Elmer, Llantrisant, UK) in the wavenumber range of (650–4000) cm^{-1}.

The insoluble fraction was determined by extracting polymer samples (0.2 g) with acetone for 24 h in a Soxhlet extractor. The samples were dried until a constant weight was reached, and the yield of the insoluble fraction was calculated as the ratio between the weight of the polymer before and after extraction and drying.

The elongation at break, tensile strength, and elastic modulus was estimated by a tensile test on a Testometric M500-50CT machine (Testometric Co Ltd, Rochdale, UK) with HDFF100 grips according to the standard ISO 527-3. Samples with dimensions of (70×10×1)±0.01 mm were tested with a crosshead speed of 5 $mm \cdot min^{-1}$. Average values were calculated from 5 parallel measurements. The variation in the experimental results did not exceed 5% within the group.

The topology freezing temperature (T_v) was determined by stress relaxation experiments on an MCR302 rheometer from Anton Paar (Graz, Austria). The samples were equilibrated with the selected measurement temperature (140–200 °C) for 20 min and a 5% step strain was applied and the decreasing stress was recorded over time.

The glass transition temperature (T_g) was determined by dynamic mechanical thermal analysis (DMTA) with an Anton Paar MCR302 rheometer (Graz, Austria). Samples with dimensions of (10×10×1)±0.01 mm were tested in a shear mode from -20 to 130 °C at a rate of 2 $°C \cdot min^{-1}$. T_g was defined as the maximum of the tanδ curve peak.

The thermal stability of the polymers was determined with a Perkin–Elmer TGA 4000 thermogravimetric analyzer (TGA) (Llantrisant, UK) with a heating rate of 20 $°C \cdot min^{-1}$ and a nitrogen flow rate of 100 $ml \cdot min^{-1}$.

2.4. DLP 3D printing

DLP 3D printing was performed on an Asiga PICO2 39 UV (Sydney, Australia) printer with a 385 nm LED UV light source. The first layer of 220 μm was exposed for 8 s and the other layers with a height of 100 μm were irradiated for 1 s. The structures of 'Benchy' and 'Marvin' were printed as they are specifically designed to test the accuracy and capabilities of 3D printers and photo-resins [25].

2.5. Self-healing experiments

UV-cured samples with (70×10×1)±0.01 mm dimensions were cut into two equal pieces, then brought in contact with each other, and heated at 200 °C for

1 h. Rejoined samples were mechanically tested with a Testometric M500-50CT machine (Testometric Co Ltd, Rochdale, UK).

The scratch repairing tests were performed by scratching the UV-cured vitrimer sample with a razor blade and curing at 200 °C for 1 h and monitoring with an Olympus BX41 optical microscope (Microscope Central, Feasterville, PA, USA).

2.6. Shape memory experiments

For shape memory experiments, the 'butterfly' sample (27×18×1)±0.01 mm) was prepared by DLP printing of the 9HPPA resin on an Asiga PICO2 39 UV printer (Sydney, Australia). Two-way shape memory experiments were carried out with a UV-cured sample with the dimensions of (70×10×1)±0.01 mm and a 'butterfly' sample. The first shape was obtained by heating the sample at 80 °C (above T_v), transforming it into the desired shape, and cooling it to 40 °C (above T_g). The second shape was obtained by heating the sample at 80 °C (above T_v) due to transforming and cooling the sample below room temperature with an ice bath. By heating again, the permanent shape was regained.

The shape recovery ratio was calculated as the ratio between the lengths of the polymer in different stages of shape memory [37]. First, the sample was heated at 80 °C (above T_v) and elongated by applying force. When in the fixing stage, the sample was cooled down to room temperature with the load applied and the tensile load was released. Finally, the deformed sample was heated to 80 °C to allow the length to recover (Equation (1)).

$$RR = \frac{L_f - L}{L_f - L_0} \cdot 100 \quad (1)$$

where RR is the shape recovery ratio [%], L_0 is the original sample length [cm], L_f is the length of the sample in the fixing stage when the tensile load is released [cm], L is the length of the sample in the recovery stage when heated at 80 °C [cm].

2.7. Recyclability experiments

The chemical degradable property was tested by immersing the samples (0.1 g) in vials with ethylene glycol (5 ml) at 200 °C. Samples were taken every hour, dried and weighed. The relative weight was calculated as the difference between the mass before and after degradation.

2.8. Reprocessability experiments

The UV-cured samples were ground into a fine powder, placed between stainless steel plates with a size of (400×400)±0.01 mm (Labtech Engineering Company Ltd, Thailand) and heated at 180 °C for 1 h at a pressure of 5 MPa. After being cooled to room temperature, the recycled samples were trimmed into a rectangular shape of (70×10×1)±0.01 mm. The remolded samples were mechanically tested with a Testometric M500-50CT machine (Testometric Co Ltd, Rochdale, UK). Average values were calculated from 5 parallel measurements. The variation in the experimental results did not exceed 5% within the group.

3. Results and discussions

3.1. Selection of the resin for vitrimer synthesis

The rheological parameters are important in the optical 3D printing process as they describe the curing rate, viscosity, and shrinkage when the resin transits from liquid to solid, and the rigidity of the final 3D printed object [38]. Thus, real-time photorheometry is now being investigated as a tool for understanding the behavior of the resin during the curing process. Viscosity determines the capacity of the resin to renew the feedstock material once the platform moves to form a new layer, and conventional 3D printing resins generally have a viscosity in the range of (200–1500) mPa·s [39]. While the viscosity determined for the glycerol and soybean oil-based resins was in the range of (184–24 862) mPa·s (Table 1) and was reduced with increasing the amount of HPPA. Importantly, the viscosities of the resins showed no significant changes after 3 months of storage in the dark. Rheological parameters such as the storage modulus (G'), the loss modulus (G''), the complex viscosity (η^*), and the shrinkage of the glycerol and soybean oil-based resins are collected in Table 2. The G' modulus of 0HPPA containing only AESO was 26.57 MPa and the G' modulus of 10HPPA containing only HPPA was 19.35 MPa, while the values of the other resins were similar to that of 9HPPA and no significant influence related to the amount of HPPA was observed. This was due to the plastification effect of HPPA that predetermined that the G' modulus that corresponds to the rigidity of 10HPPA was the lowest. Although the G'' modulus, which corresponds to the energy dissipated as heat, representing

Table 2. Real-time photorheometry data of glycerol- and soybean oil-based resins.

Resin	Storage modulus, G' [MPa]	Loss modulus, G'' [MPa]	Complex viscosity, η^* [MPa·s]	Shrinkage [%]
0HPPA	26.57±2.19	4.87±0.85	0.45±0.01	3.0±0.0
1HPPA	23.85±2.95	6.19±2.18	0.39±0.05	6.5±0.5
2HPPA	27.60±1.10	8.36±0.63	0.46±0.01	6.5±0.5
3HPPA	25.45±1.25	6.39±0.18	0.42±0.02	7.5±0.5
4HPPA	25.60±0.60	11.23±2.48	0.45±0.01	7.5±0.5
5HPPA	23.75±0.65	12.40±0.40	0.43±0.01	9.5±1.0
6HPPA	22.10±0.60	11.30±0.60	0.40±0.01	6.5±0.5
7HPPA	23.45±0.85	12.90±1.20	0.35±0.00	7.5±0.5
8HPPA	24.40±1.30	14.20±4.41	0.46±0.02	6.5±0.5
9HPPA	23.25±1.55	13.34±3.56	0.43±0.01	6.5±0.5
10HPPA	19.35±0.45	16.00±2.00	0.40±0.02	7.5±0.5

the viscous part [38] showed the opposite results, as the resin 10HPPA had the highest G'' modulus of 16 MPa. η^* values which represent the resistance to flow as a function of the angular frequency of all resins based on glycerol and soybean oil were in the same range (0.35–0.45 mPa·s), while the shrinkage of the resin 10HPPA (7.5%) resin was greater compared to the AESO resin 0HPPA (3.0%) due to the lower viscosity and the tgel values did not influence since the gelation of all resin began after 2 s of irradiation. Based on data from the published literature, resins for vitrimer synthesis by optical 3D printing frequently consist of the ratio of 9:1 from the monomer and the cross-linker [23, 24], therefore, the storage modulus G' describes the rigidity *versus* the irradiation time of resins without HPPA (0HPPA), with 90 wt% of HPPA (9HPPA), and without AESO (10HPPA) are presented in Figure 2. The resin 9HPPA exhibited the intermediate G' modulus value after 2 min of irradiation (23.25 MPa).

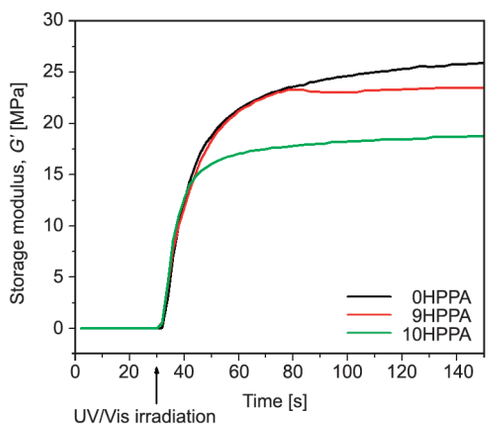

Figure 2. Curves of the storage modulus G' versus irradiation time of resins without HPPA (0HPPA), with 90 wt% of HPPA (9HPPA), and without AESO (10HPPA).

Tensile testing and extraction of polymer samples were performed to investigate the mechanical properties and the yield of the insoluble fraction of the UV-cured resins (Figure 3). Polymer rigidity is

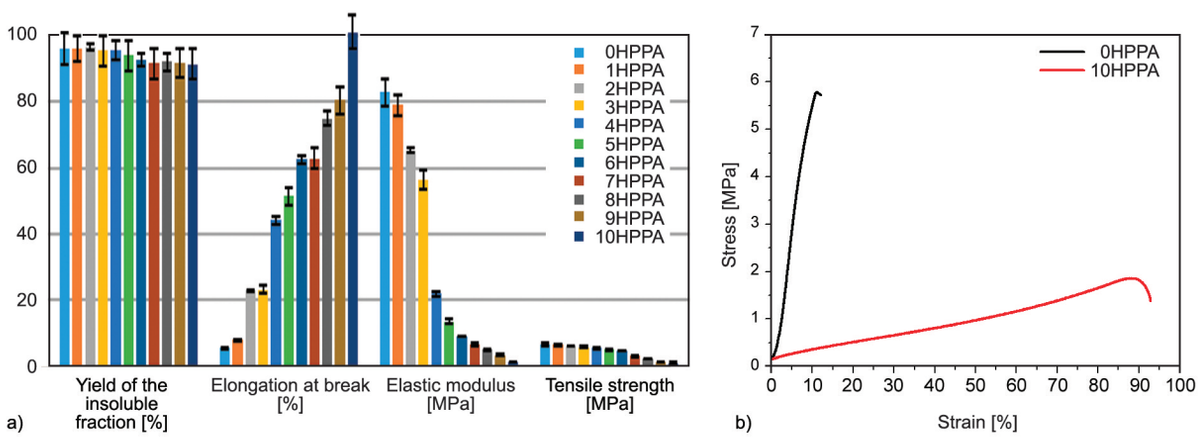

Figure 3. Yield of the insoluble fraction and mechanical characteristics of the polymers based on glycerol and soybean oil (a) and stress-strain curves of the polymers 0HPPA and 10HPPA (b).

important when planning applications in the industry, and rigid as well as flexible polymers are used in various areas depending on the needs of the 3D printed structure. The HPPA monomer with the glycerol fragment was determined to act as a plasticizer [19] as it lowered the values of tensile strength, elastic modulus, of the insoluble fraction and increased the values of elongation at break. The polymer yield having the highest amount of HPPA had the lowest values of tensile strength, yield of the insoluble fraction and elastic modulus (1.39 MPa, 91.79% and 3.45 MPa) and the highest value of elongation at break (80.47%).

After evaluation of the rheological and mechanical characteristics of the polymers, it was decided to select the resin 9HPPA for vitrimer synthesis with the lowest amount of AESO and the highest amount of HPPA, which ensures the highest amount of hydroxyl and ester groups that are beneficial for transesterification reactions. Furthermore, the viscosity of the resin (332 mPa·s) (Table 1) was suitable for the formation of 3D structures using DLP. The chemical structure of the 9HPPA uncured, photocured, and thermally post-cured resin at 200 °C was confirmed by FT-IR spectroscopy (Figure 4). The intensities of the OH and C=O groups at 3434 and 1732 cm^{-1} remain constant in the photocured polymer spectrum in comparison with the spectra of the uncured resin, which is essential for the transesterification reaction. The intensity of the C=C group signal, which was present at 1599 cm^{-1} was reduced after photopolymerization. After post-curing at 200 °C, a decrease in OH groups was observed due to hydrogen bonding formation. Stress relaxation experiments were performed to determine the topology freezing temperature (T_v) of the resin 9HPPA. The thermal properties

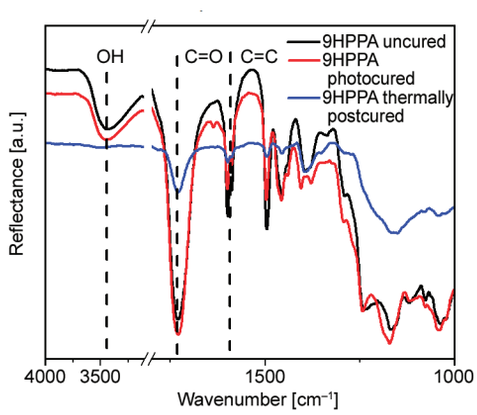

Figure 4. FTIR spectra of the uncured, photocured, and thermally postcured resin 9HPPA.

of the polymer 9HPPA and the post-cured vitrimer 9HPPAV at 200 °C were compared with the neat AESO polymer and the neat HPPA polymer (0HPPA and 10HPPA, respectively). Vitrimeric abilities, such as shape memory, self-healing, recycling, and reprocessing properties, were investigated.

3.2. Thermal properties

The thermal characteristics obtained by DMTA and TGA analysis of polymers based on glycerol and soybean oil are summarized in Table 3. The thermal properties of the UV-cured polymer 9HPPA were compared with the polymer 0HPPA only with the fragments of AESO in the structure, polymer 10HPPA containing the fragments of HPPA, and the vitrimer 9HPPAV, which was obtained by post-curing the 9HPPA at 200 °C for 4 h. The incorporation of HPPA into the network led to the obtainment of the polymer with a higher T_g temperature (23 °C) compared to the polymer with flexible AESO chains (0 °C). However, the highest values of T_g, G_r', $T_{dec\text{-}10\%}$, and char yield (53 °C, 0.15 MPa, 335 °C, and 16.5%, respectively) were obtained when the UV-cured 9HPPA polymer was post-cured at 200 °C. This was due to the highest yield of the insoluble fraction (99.5%) after extraction with acetone, which was chosen as a solvent due to its ability to dissolve both polar and minor polar substances, while other solvents can only dissolve one or the other [40]. The curves of the storage modulus *G′ versus* temperature obtained from the DMTA analysis are presented in Figure 5a. It can be seen that the UV-cured polymer 10HPPA has a peak at about 20 °C meaning that the monomer HPPA provides crystallinity to the network due to the presence of benzene rings [41], however, the polymer is more amorphous as it gradually softened and did not melt with increasing temperature. Although glycerol is one of the most studied glass formers, it also has an extremely low tendency to crystallize [42]. The more clearly apparent peak can be seen in the curve of post-cured vitrimer 9HPPAV and the *G′* modulus remained the same as the temperature increased, meaning the network of vitrimer is more semicrystalline when amorphous with more uniformly packed molecules. Two peaks have been observed in the curves of tanδ versus temperature (Figure 5b). The lower temperature peak contributes to the β-relaxation process observed below T_g, which is associated with the polymer backbone and involves local motions of the polymer chain backbone that do not

Table 3. Yield of the insoluble fraction, thermal, and thermomechanical characteristics of polymers.

Polymer	The yield of the insoluble fraction[1] [%]	DMTA		TGA	
		T_g[2] [°C]	G_r'[3] [MPa]	$T_{dec\text{-}10\%}$[4] [°C]	Char yield[5] [%]
0HPPA	96.3±0.2	0	0.24	312	7.3
9HPPA	91.8±0.1	23	0.06	289	13.1
9HPPAV	99.5±0.8	53	0.15	335	16.5
10HPPA	91.4±0.2	23	0.04	265	14.1

[1]After 24 h of Soxhlet extraction with acetone,
[2]Glass transition temperature determined by DMTA,
[3]Storage shear modulus of cured resins in the rubbery plateau region,
[4]Temperature at a weight loss of 10% obtained from TGA curves,
[5]From TGA curves.

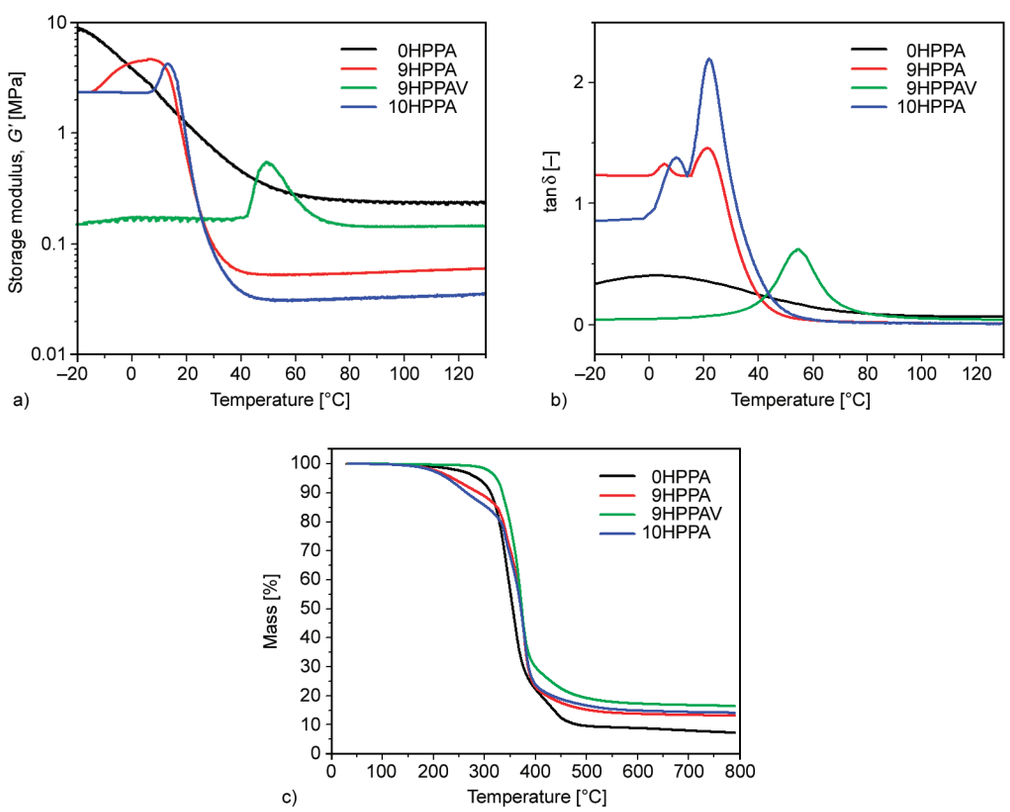

Figure 5. Curves of the storage modulus *G' versus* temperature (a), curves of tan δ *versus* temperature (b), and thermogravimetric curves of polymers based on glycerol and soybean oil (c).

require cooperative motion of the surrounding chains and is a precursor for the primary α-relaxation process (T_g) [43]. The thermal decomposition of the UV-cured polymer 9HPPA proceeded in two steps, while the thermal degradation of the vitrimer 9HPPAV proceeded in one step (Figure 5c), which confirmed a densely cross-linked network.

3.3. Relaxation of the stress of the vitrimer

Thermosets have permanent covalent bonds in their network, which leads to difficulties in stress relaxation. While vitrimers with dynamic bonds can rearrange the network and alleviate the relaxation of internal stress caused by deformation [44]. Therefore, topology rearrangements were investigated by measuring the stress relaxation of sample 9HPPA (Figure 6) and a topology freezing transition temperature (T_v) was determined at which the transition from viscoelastic solid to viscoelastic liquid occurs. Stress relaxation experiments were carried out at temperatures (160–200 °C) and thermal degradation was avoided, as the thermal stability of the 9HPPA sample is above 200 °C (Figure 5c). The relaxation time (τ^*) is the time the modulus relaxes to 1/e of its value [45]. With increasing temperature, the relaxation time of the 9HPPA decreased from 172.45 to 11.5 min

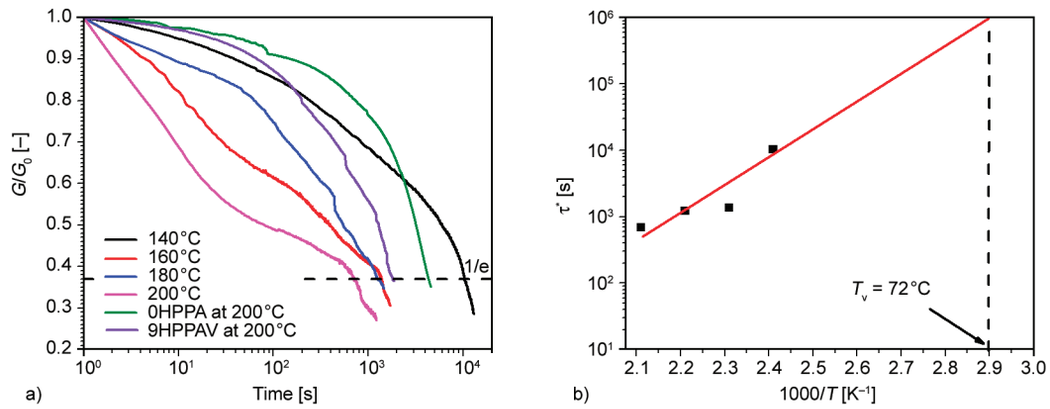

Figure 6. Stress relaxation curves versus the time of 9HPPA, 0HPPA, and the 9HPPAV (a) and Arrhenius plot of relaxation times (b).

due to dynamic bond exchange and chain diffusion. The relaxation time of 0HPPA at 200 °C was 71.12 min, which shows that more ester groups need more time to relax. Furthermore, 9HPPAV at 200 °C needed 30.18 min to relax, which is more compared to photocured 9HPPA showing the additional formation of hydrogen bonds during curing at 200 °C that results in a decrease in OH groups that could not participate in transesterification reactions (Figure 4). The topology freezing temperature (T_v) can be determined from the Arrhenius curves for relaxation times of 10^6 s [9]. Therefore, the T_v value of 9HPPA was obtained by extrapolating the data to a relaxation time of 10^6 s and was 72 °C (Figure 6b).

3.4. DLP 3D printing and shape memory properties

DLP 3D printing has advantages such as high resolution and accuracy, good surface finish, high fabrication speed, and is attractive for the formation of objects that need to have the mentioned properties [46]. Therefore, the accurate structures 'Benchy' and 'Marvin' with small details and smooth surface finishing were formed to show the suitability of the resin 9HPPA for DLP 3D printing (Figure 7a).

Two-way shape memory polymers can be used in the application of reversible actuation as artificial muscles and actuators, as they can transit between two different shapes spontaneously and reversibly when heating or cooling is applied [47]. Flexible AESO chains and free hydroxyl groups of the UV-cured polymer 9HPPA provide plasticity that could impart shape memory properties [48]. Therefore, the two-way shape memory cycle of the DLP 3D printed 'butterfly' sample and the UV-cured rectangular sample is shown in Figures 7b and 7c. The procedure consisted of transforming the samples above T_v and fixing above and below T_g. The permanent shape of the printed and UV-cured samples was changed by heating above I_v at 80 °C and applying the external force for deformation. The first shape was fixed by cooling the sample down above T_g to 40 °C. The second shape of a 'butterfly' was obtained by cooling down the sample below T_g to 0 °C and fixing the wings to the desired shape. The rectangular shape obtained the second desired 'spiral' shape only by transforming at above T_v and cooling down the sample below T_g. After being heated above the T_v, the samples completely recovered to the permanent shape, indicating an excellent shape memory property. Both the UV-cured rectangular and DLP 3D printed 'butterfly' sample showed a shape recovery ratio (RR) of 100% meaning that the samples are able to recover their original length.

3.5. Self-healing properties

To investigate the self-healing properties of vitrimer 9HPPAV, the UV-cured sample 9HPPA was cut and rejoined at 200 °C for 1 h, and the stress-strain curves of the samples are presented in Figure 8. Mechanical properties were improved after a thermal treatment, indicating excellent repairability and weldability of the cured sample. The elastic modulus of the thermally treated sample 9HPPAV was 134 MPa, which is 38 times higher compared to the UV-cured sample 9HPPA, and elongation at break was reduced by approximately 3 times to 30%. This was due to topological rearrangements and additional formation of hydrogen bonding during prolonged treatment at 200 °C that resulted in a decrease in OH groups (Figure 4).

Scratch-repairing test was performed to verify the repairability as self-healing of the UV-cured sample

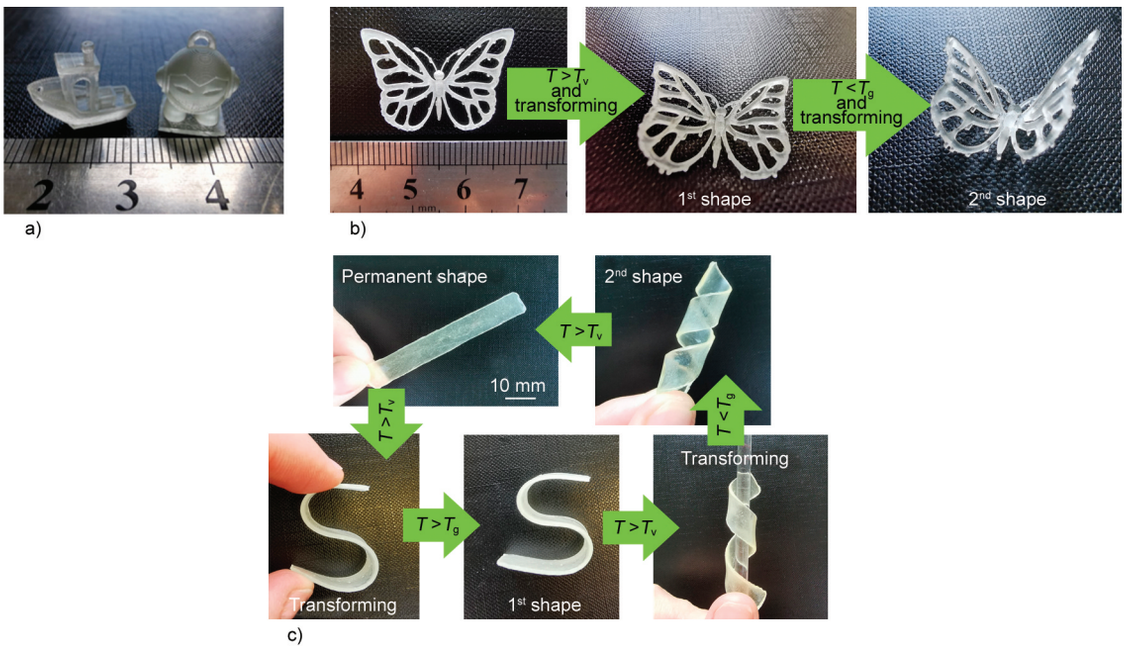

Figure 7. Photographs expressing DLP printing of 'Benchy' and 'Marvin' structures (a) and monitoring the shape memory behavior of 9HPPA: of DLP printed 'butterfly' sample (b) and UV-cured rectangular sample (c).

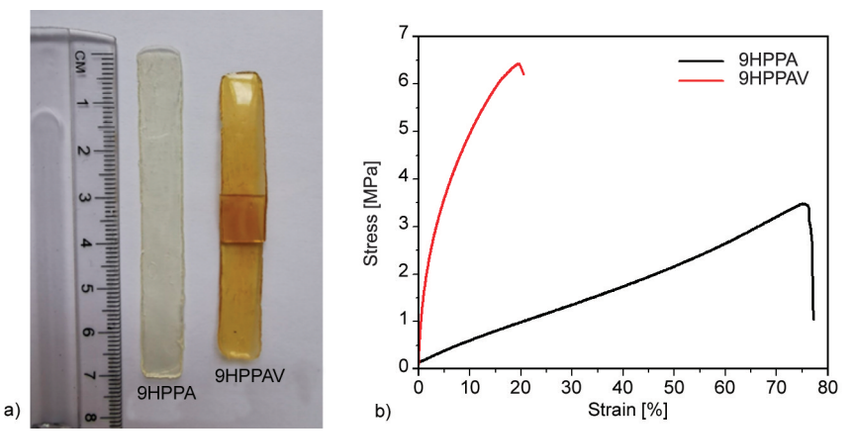

Figure 8. Photograph (a) and stress-strain curves (b) of the UV-cured 9HPPA sample and the vitrimer 9HPPAV after repair at 200 °C for 1 h.

9HPPA at high temperatures should occur due to dynamic transesterification reactions. Images of the scratched UV-cured sample 9HPPA with a razor blade and repaired at 200 °C for 1 h are shown in Figure 9. Self-healing with an efficiency of 47% was obtained as the ratio between the width of the repaired sample and the width of the initial sample. The sufficiently low T_g value provided active chain mobility at a temperature of 200 °C [44].

3.6. Recyclability

Polymeric products need to be degraded after the end of their use when they do not have useful properties. This would reduce the negative impact on environmental health, which is the main idea of green chemistry and chemical engineering [49]. The chemical recycling of thermosets into soluble products is usually carried out by catalysis at high temperatures using pressure to recycle the network [50]. While the chemical recycling of vitrimers at elevated temperatures is carried out more simply through alcoholysis due to dynamic bond exchange reactions [13]. Therefore, the chemical degradation of the sample 9HPPA was performed with ethylene glycol (Figure 10a) and the curve of weight loss of 9HPPA *versus* temperature is presented in Figure 10b. After recyclability testing, the color of ethylene glycol changed from transparent to brown and the 9HPPA sample shrank, indicating that the transesterification reaction between the ester bonds of the sample 9HPPA and hydroxyl groups of ethylene glycol occurred as the cross-linked network was deconstructed and the

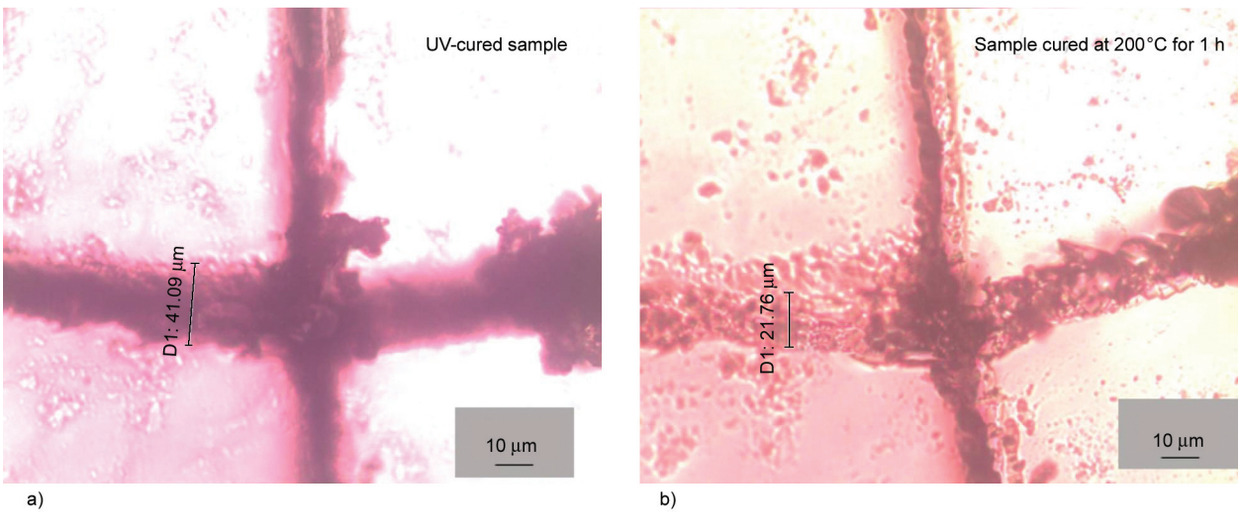

Figure 9. Scratch repair images of the UV-cured sample 9HPPA. a) UV-cured sample, b) Sample cured at 200 °C for 1 h

degraded product was dissolved in ethylene glycol. The weight of the sample decreased rapidly to 50% during the first 6 h and gradually to 10% during the 17 h and stabilized. The permanent linkages of the sample had an impact on the residue after chemical degradation. The intensities of the OH, C=C and C=O group signals at 3434, 1599 and 1732 cm^{-1} remained the same in the spectra of the sample 9HPPA residue after alcoholysis and dissolved in ethylene glycol, since the rearrangement of the cross-linked network occurred via dynamic transesterification (Figure 10c).

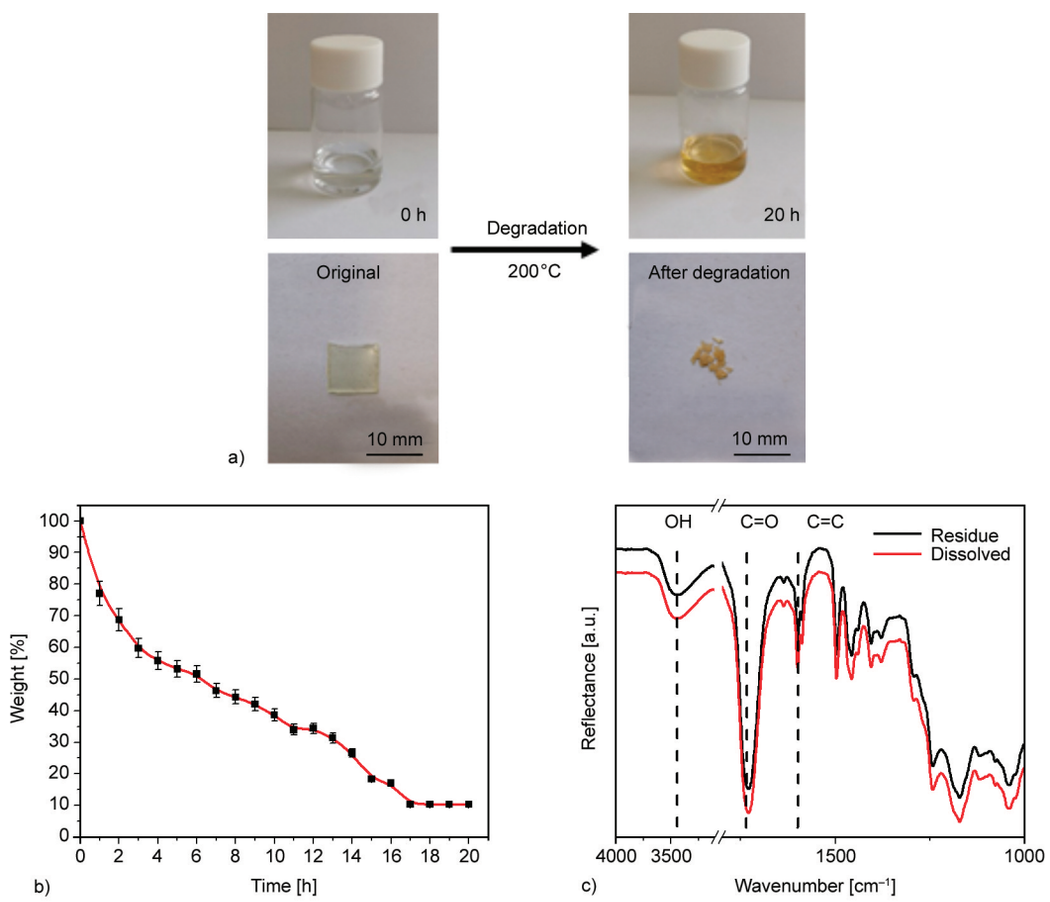

Figure 10. Photograph expressing the chemical degradation experiment (a), the weight loss of 9HPPA versus temperature (b), and the FTIR spectra of the sample residue after alcoholysis and dissolved in ethylene glycol (c).

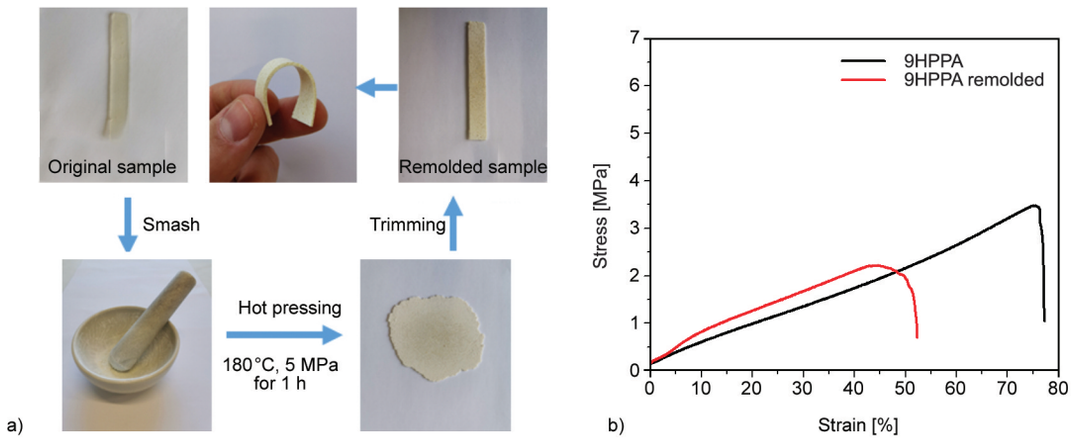

Figure 11. Photograph expressing the reprocessability experiment (a) and stress-strain curves of the UV-cured and remolded sample 9HPPA (b).

3.7. Reprocessability

To demonstrate the reprocessability of the UV-cured sample 9HPPA, the grounded fine powder was heated at 180 °C for 1 h under a pressure of 5 MPa and the remolded samples were obtained (Figure 11a). After reprocessing, the sample retained its elasticity. The stress-strain curves of the UV-cured sample 9HPPA and the remolded sample are shown in Figure 11b. The remolded sample exhibited a higher elastic modulus of 6.86 MPa compared to the original sample with an elastic modulus of 3.45 MPa. However, the sample could not be fully restored as it showed lower values of tensile strength and elongation at break compared to the original sample (0.43 MPa, 48.10% and 1.39 MPa, 80.47%, respectively). A recycling efficiency of 31% was calculated as the ratio of the tensile strength of the recycled and original samples.

4. Conclusions

Glycerol- and soybean oil-based resins were designed using an environmentally friendly strategy by mixing the monomers in different ratios with a photoinitiator and a transesterification catalyst and applying irradiation under solvent-free conditions. Acrylated epoxidized soybean oil was used in UV-curable resins for the synthesis of vitrimer for the first time. The resin containing the highest amount of functionalized glycerol was selected for the vitrimer synthesis and DLP 3D printing as a real-time photorheometric study showed that the rigidity and viscosity of the resins were reduced with increasing amount of glycerol-based monomer and the selected resin contained the highest amount of hydroxyl and ester groups that are beneficial for transesterification reactions. The dynamic network of UV-cured material showed stress relaxation at elevated temperatures and a topology freezing temperature of 72 °C. Acrylated epoxidized soybean oil was found to be a suitable cross-linker in the UV-curing reactions with 2-hydroxy-2-phenoxypropyl acrylate as it led to reach shape memory, self-healing, reprocessability, and recyclability properties. Flexible chains of acrylated epoxidized soybean oil and free hydroxyl groups of the UV-cured sample imparted shape memory properties. Thermal and mechanical properties after vitrimer welding were improved due to the additional formation of hydrogen bonds during prolonged treatment at 200 °C. The synthesized vitrimer showed self-healing and reprocessability with an efficiency of 47 and 31 %, respectively, and was degraded by alcoholysis. The vitrimeric abilities of the synthesized vitrimer could contribute to recyclability and decrease production costs because the vitrimer could partially repair cracks and defects, change the permanent shape to the new one, and, because of weldability, could have a complex design from several parts. The synthesized vitrimer could be applied in reversible actuation as artificial muscles and actuators, where transits between two shapes are required.

Acknowledgements

This project has received funding from European Social Fund (project No. 09.9.9-LMT-K-712-23-0088) under grant agreement with the Research Council of Lithuania (LMTLT).

References

[1] Guerre M., Taplan C., Winne J. M., du Prez F. E.: Vitrimers: Directing chemical reactivity to control material properties. Chemical Science, **11**, 4855–4870 (2020). https://doi.org/10.1039/d0sc01069c

[2] Huang S., Kong X., Xiong Y., Zhang X., Chen H., Jiang W., Niu Y., Xu W., Ren C.: An overview of dynamic covalent bonds in polymer material and their applications. European Polymer Journal, **141**, 110094 (2020). https://doi.org/10.1016/j.eurpolymj.2020.110094

[3] Zheng J., Png Z. M., Ng S. H., Tham G. X., Ye E., Goh S. S., Loh X. J., Li Z.: Vitrimers: Current research trends and their emerging applications. Materials Today, **51**, 586–625 (2021). https://doi.org/10.1016/j.mattod.2021.07.003

[4] Memon H., Wei Y., Zhu C.: Recyclable and reformable epoxy resins based on dynamic covalent bonds – Present, past, and future. Polymer Testing, **105**, 107420 (2022). https://doi.org/10.1016/j.polymertesting.2021.107420

[5] Alabiso W., Schlögl S.: The impact of vitrimers on the industry of the future: Chemistry, properties and sustainable forward-looking applications. Polymers, **12**, 1660 (2020). https://doi.org/10.3390/polym12081660

[6] Lucherelli M. A., Duval A., Avérous L.: Biobased vitrimers: Towards sustainable and adaptable performing polymer materials. Progress in Polymer Science, **127**, 101515 (2022). https://doi.org/10.1016/j.progpolymsci.2022.101515

[7] Winne J. M., Leibler L., du Prez F. E.: Dynamic covalent chemistry in polymer networks: A mechanistic perspective. Polymer Chemistry, **10**, 6091–6108 (2019). https://doi.org/10.1039/c9py01260e

[8] Montarnal D., Capelot M., Tournilhac F., Leibler L.: Silica-like malleable materials from permanent organic networks. Science, **334**, 965–968 (2011). https://doi.org/10.1126/science.1212648

[9] Capelot M., Unterlass M. M., Tournilhac F., Leibler L.: Catalytic control of the vitrimer glass transition. ACS Macro Letters, **1**, 789–792 (2012). https://doi.org/10.1021/mz300239f

[10] Tellers J., Pinalli R., Soliman M., Vachon J., Dalcanale E.: Reprocessable vinylogous urethane cross-linked polyethylene *via* reactive extrusion. Polymer Chemistry, **10**, 5534–5542 (2019). https://doi.org/10.1039/C9PY01194C

[11] Zych A., Tellers J., Bertolacci L., Ceseracciu L., Marini L., Mancini G., Athanassiou A.: Biobased, biodegradable, self-healing boronic ester vitrimers from epoxidized soybean oil acrylate. ACS Applied Polymer Materials, **3**, 1135–1144 (2021). https://doi.org/10.1021/acsapm.0c01335

[12] Freed K. F.: The descent into glass formation in polymer fluids. Accounts of Chemical Research, **44**, 194–203 (2011). https://doi.org/10.1021/ar100122w

[13] Liu T., Zhao B., Zhang J.: Recent development of repairable, malleable and recyclable thermosetting polymers through dynamic transesterification. Polymer, **194**, 122392 (2020). https://doi.org/10.1016/j.polymer.2020.122392

[14] Lossada F., Guo J., Jiao D., Groeer S., Bourgeat-Lami E., Montarnal D., Walther A.: Vitrimer chemistry meets cellulose nanofibrils: Bioinspired nanopapers with high water resistance and strong adhesion. Biomacromolecules, **20**, 1045–1055 (2018). https://doi.org/10.1021/acs.biomac.8b01659

[15] Moazzen K., Rossegger E., Alabiso W., Shaukat U., Schlögl S.: Role of organic phosphates and phosphonates in catalyzing dynamic exchange reactions in thiol-click vitrimers. Macromolecular Chemistry and Physics, **222**, 2100072 (2021). https://doi.org/10.1002/macp.202100072

[16] Rossegger E., Höller R., Reisinger D., Fleisch M., Strasser J., Wieser V., Griesser T., Schlögl S.: High resolution additive manufacturing with acrylate based vitrimers using organic phosphates as transesterification catalyst. Polymer, **221**, 123631 (2021). https://doi.org/10.1016/j.polymer.2021.123631

[17] Rossegger E., Höller R., Reisinger D., Strasser J., Fleisch M., Griesser T., Schlögl S.: Digital light processing 3D printing with thiol–acrylate vitrimers. Polymer Chemistry, **12**, 639–644 (2021). https://doi.org/10.1039/d0py01520b

[18] Yang F., Hanna M. A., Sun R.: Value-added uses for crude glycerol – A byproduct of biodiesel production. Biotechnology for Biofuels, **5**, 13 (2012). https://doi.org/10.1186/1754-6834-5-13

[19] Monteiro M. R., Kugelmeier C. L., Pinheiro R. S., Batalha M. O., da Silva César A.: Glycerol from biodiesel production: Technological paths for sustainability. Renewable and Sustainable Energy Reviews, **88**, 109–122 (2018). https://doi.org/10.1016/j.rser.2018.02.019

[20] Kasetaite S., Ostrauskaite J., Grazuleviciene V., Svediene J., Bridziuviene D.: Photocross-linking of glycerol diglycidyl ether with reactive diluents. Polymer Bulletin, **72**, 3191–3208 (2015). https://doi.org/10.1007/s00289-015-1461-x

[21] Kasetaite S., Ostrauskaite J., Grazuleviciene V., Bridziuviene D., Rainosalo E.: Biodegradable glycerol-based polymeric composites filled with industrial waste materials. Journal of Composite Materials, **51**, 4029–4039 (2017). https://doi.org/10.1177/0021998317697809

[22] Kasetaite S., Ostrauskaite J., Grazuleviciene V., Bridziuviene D., Budreckiene R., Rainosalo E.: Biodegradable photocross-linked polymers of glycerol diglycidyl ether and structurally different alcohols. Reactive and Functional Polymers, **122**, 42–50 (2018). https://doi.org/10.1016/j.reactfunctpolym.2017.11.005

[23] Zhang B., Kowsari K., Serjouei A., Dunn M. L., Ge Q.: Reprocessable thermosets for sustainable three-dimensional printing. Nature Communications, **9**, 1831 (2018). https://doi.org/10.1038/s41467-018-04292-8

[24] Li H., Zhang B., Wang R., Yang X., He X., Ye H., Cheng J., Yuan C., Zhang Y-F., Ge Q.: Solvent-free upcycling vitrimers through digital light processing-based 3D printing and bond exchange reaction. Advanced Functional Materials, **32**, 2111030 (2022). https://doi.org/10.1002/adfm.202111030

[25] Skliutas E., Lebedevaite M., Kasetaite S., Rekštytė S., Lileikis S., Ostrauskaite J., Malinauskas M.: A bio-based resin for a multi-scale optical 3D printing. Scientific Reports, **10**, 9758 (2020). https://doi.org/10.1038/s41598-020-66618-1

[26] Tremblay-Parrado K-K., García-Astrain C., Avérous L.: Click chemistry for the synthesis of biobased polymers and networks derived from vegetable oils. Green Chemistry, **23**, 4296–4327 (2021). https://doi.org/10.1039/D1GC00445J

[27] Mustapha R., Rahmat A. R., Majid R. A., Mustapha S. N. H.: Vegetable oil-based epoxy resins and their composites with bio-based hardener: A short review. Polymer-Plastics Technology and Materials, **58**, 1311–1326 (2019). https://doi.org/10.1080/25740881.2018.1563119

[28] Güner F. S., Yağci Y., Erciyes A. T.: Polymers from triglyceride oils. Progress in Polymer Science, **31**, 633–670 (2006). https://doi.org/10.1016/j.progpolymsci.2006.07.001

[29] Lebedevaite M., Talacka V., Ostrauskaite J.: High bionewable content acrylate photocurable resins for DLP 3D printing. Journal of Applied Polymer Science, **138**, e50233 (2021). https://doi.org/10.1002/app.50233

[30] Lebedevaite M., Gineika A., Talacka V., Baltakys K., Ostrauskaite J.: Development and optical 3D printing of acrylated epoxidized soybean oil-based composites with functionalized calcium silicate hydrate filler derived from aluminium fluoride production waste. Composites Part A: Applied Science and Manufacturing, **157**, 106929 (2022). https://doi.org/10.1016/j.compositesa.2022.106929

[31] Tran T-N., Di Mauro C., Graillot A., Mija A.: Chemical reactivity and the influence of initiators on the epoxidized vegetable oil/dicarboxylic acid system. Macromolecules, **53**, 2526–2538 (2020). https://doi.org/10.1021/acs.macromol.9b02700

[32] Di Mauro C., Malburet S., Genua A., Graillot A., Mija A.: Sustainable series of new epoxidized vegetable oil-based thermosets with chemical recycling properties. Biomacromolecules, **21**, 3923–3935 (2020). https://doi.org/10.1021/acs.biomac.0c01059

[33] Altuna F. I., Pettarin V., Williams R. J. J.: Self-healable polymer networks based on the cross-linking of epoxidised soybean oil by an aqueous citric acid solution. Green Chemistry, **15**, 3360–3366 (2013). https://doi.org/10.1039/C3GC41384E

[34] Wu J., Yu X., Zhang H., Guo J., Hu J., Li M-H.: Fully biobased vitrimers from glycyrrhizic acid and soybean oil for self-healing, shape memory, weldable, and recyclable materials. ACS Sustainable Chemistry and Engineering, **8**, 6479–6487 (2020). https://doi.org/10.1021/acssuschemeng.0c01047

[35] Green W. A.: Industrial photoinitiators: A technical guide. CRC Press, Boca Raton (2010).

[36] Navaruckiene A., Bridziuviene D., Raudoniene V., Rainosalo E., Ostrauskaite J.: Vanillin acrylate-based thermo-responsive shape memory antimicrobial photopolymers. Express Polymer Letters, **16**, 279–295 (2022). https://doi.org/10.3144/expresspolymlett.2022.22

[37] Gu S., Jana S.: Effects of polybenzoxazine on shape memory properties of polyurethanes with amorphous and crystalline soft segments. Polymers, **6**, 1008–1025 (2014). https://doi.org/10.3390/polym6041008

[38] Mezger T. G.: The rheology handbook. Vincentz Network, Hannover (2011).

[39] Pugh R. J., Bergstrom L.: Surface and colloid chemistry in advanced ceramics processing. CRC Press, Boca Raton (2017).

[40] Eloff J. N.: Which extractant should be used for the screening and isolation of antimicrobial components from plants? Journal of Ethnopharmacology, **60**, 1–8 (1998). https://doi.org/10.1016/s0378-8741(97)00123-2

[41] Zhang Z. P., Rong M. Z., Zhang M. Q.: Polymer engineering based on reversible covalent chemistry: A promising innovative pathway towards new materials and new functionalities. Progress in Polymer Science, **80**, 39–93 (2018). https://doi.org/10.1016/j.progpolymsci.2018.03.002

[42] Roed L. A., Gundermann D., Dyre J. C., Niss K.: Communication: Two measures of isochronal superposition. The Journal of Chemical Physics, **139**, 101101 (2013). https://doi.org/10.1063/1.4821163

[43] Smith G. D., Bedrov D.: Relationship between the α- and β-relaxation processes in amorphous polymers: Insight from atomistic molecular dynamics simulations of 1,4-polybutadiene melts and blends. Journal of Polymer Science Part B: Polymer Physics, **5**, 627–643 (2007). https://doi.org/10.1002/polb.21064

[44] Zhang J., Huang J., Zhu G., Yu X., Cheng J., Liu Z., Hu Y., Shang Q., Liu C., Hu L., Zhou Y.: Self-healing, recyclable, and removable UV-curable coatings derived from tung oil and malic acid. Green Chemistry, **23**, 5875–5886 (2021). https://doi.org/10.1039/D1GC01726H

[45] Qiu M., Wu S., Fang S., Tang Z., Guo B.: Sustainable, recyclable and robust elastomers enabled by exchangeable interfacial cross-linking. Journal of Materials Chemistry A, **6**, 13607–13612 (2018). https://doi.org/10.1039/C8TA04173C

[46] González-Henríquez C. M., Sarabia-Vallejos M. A., Rodriguez-Hernandez J.: Polymers for additive manufacturing and 4D-printing: Materials, methodologies, and biomedical applications. Progress in Polymer Science, **94**, 57–116 (2019).
https://doi.org/10.1016/j.progpolymsci.2019.03.001

[47] Jin B., Song H., Jiang R., Song J., Zhao Q., Xie T.: Programming a crystalline shape memory polymer network with thermo- and photo-reversible bonds toward a single-component soft robot. Science advances, **4**, eaao3865 (2018).
https://doi.org/10.1126/sciadv.aao3865

[48] Liang R., Yu H., Wang L., Amin B. U., Wang N., Fu J., Xing Y., Shen D., Ni Z.: Triple and two-way reversible shape memory polymer networks with body temperature and water responsiveness. Chemistry of Materials, **33**, 1190–1200 (2021).
https://doi.org/10.1021/acs.chemmater.0c03860

[49] Zhang Y.: Discussion on the development of green chemistry and chemical engineering. in 'Proceedings of the IOP Conference Series: Earth and Environmental Science, 3rd International Conference on Energy, Environment and Materials Science (EEMS 2017). Singapore' Vol. 94, 012136 (2017).
https://doi.org/10.1088/1755-1315/94/1/012136

[50] Liu T., Zhang M., Guo X., Liu C., Liu T., Xin J., Zhang J.: Mild chemical recycling of aerospace fiber/epoxy composite wastes and utilization of the decomposed resin. Polymer Degradation and Stability, **139**, 20–27 (2017).
https://doi.org/10.1016/j.polymdegradstab.2017.03.017